Affiliation: Independent Researcher *Email:* bierrenbach85@gmail.com

Abstract

This paper introduces the Regenerative Gravity and Spatial Homeostasis Equation (GRHE), a novel framework challenging cosmic expansion, dark matter, and dark energy. GRHE proposes a static universe governed by a scalar field $\Psi(r, t)$ and the golden ratio ($\phi \approx 1.618$). It defines a distance metric (r_{GRHE}) and a quantum redshift mechanism, tested across 20 scenarios (e.g., Milky Way-Andromeda, CMB, Type Ia supernovae), yielding an average error of 1.63% (1.11% for cosmological scales with a hybrid Fibonacci/ϕ-scaling approach). GRHE is comparable to LambdaCDM's typical 1–2% error while eliminating dark components. It extends to black holes, lensing, and advanced cosmological tests (see Supplementary Material V), offering a unified alternative to LambdaCDM.

Keywords: GRHE, golden ratio, cosmology, redshift, scalar field, functional equilibrium
This manuscript is accompanied by Supplementary Materials expanding GRHE's validation to 20 scenarios, including baryon acoustic oscillations, galaxy rotation, gravitational lensing, and Type Ia supernovae, with further cosmological tests in Supplementary Material V.

A New Cosmological Framework: The Regenerative Gravity and Spatial Homeostasis Equation with Golden Ratio Integration

Jorge Bierrenbach

April 10, 2025

1 Introduction

The Lambda Cold Dark Matter (LambdaCDM) model relies on expansion, dark matter, and dark energy, yet lacks direct evidence for these components [1]. Challenges like the "Hubble tension" [2] and baryon acoustic oscillation (BAO) discrepancies [3] underscore the need for alternatives. The Regenerative Gravity and Spatial Homeostasis Equation (GRHE) posits a static, organic universe governed by a scalar field $\Psi(r,t)$, using the golden ratio ($\phi \approx 1.618$) to unify metrics. This paper presents GRHE's philosophy, methodology, tests, and a functional cosmic map.

2 Philosophical Foundations

GRHE views the universe as a self-regulating system, inspired by autopoiesis [4] and process philosophy [5]:

- **Structural Unity**: The golden ratio, seen in galactic spirals [6], encodes $\Psi(r,t)$.
- **Functional Equilibrium**: Phenomena arise from balance via $\vec{F}(r,t) = -\nabla\Psi(r,t)$.

See Appendix C for details.

2.1 The Logic of the Cosmos — GRHE and Hierarchical Patterns

GRHE models the universe as a dynamic system where $\Psi(r,t)$ drives equilibrium. The golden ratio is embedded in the coupling constant k_0' (Appendix D), with $\gamma \approx \phi^{2.1} \cdot \left(\frac{c/H_0}{l_P}\right)^{0.7386}$.

2.1.1 $\Psi(r,t)$: The Universal Code

The scalar field evolves as:

$$\frac{\partial\Psi}{\partial t} = \lambda\rho - \eta\nabla\cdot\vec{F} + \kappa\dot{M} + \mu\Phi, \tag{1}$$

balancing density (ρ), force divergence ($\nabla\cdot\vec{F}$), mass flux ($\dot{M}$), and potential (Φ).

Table 1: Analogy between GRHE components and biological systems.

GRHE Component	Meaning	Biological Analogy	Cosmic Function
$\Psi(r,t)$	Scalar field	Regulatory mechanism	Encodes equilibrium
$\nabla\Psi(r,t)$	Gradient	Signal transduction	Drives responses
$\vec{F}(r,t)$	Force response	Regulation	Restores balance
k (constant)	Sensitivity	Feedback control	Modulates intensity

2.1.2 The Fibonacci Sequence: The Code of Natural Harmony

The Fibonacci sequence:

$$F_n = F_{n-1} + F_{n-2}, \quad F = (0, 1, 1, 2, 3, 5, 8, 13, 21, \dots), \tag{2}$$

converges to $\phi \approx 1.618$, seen in galactic spirals and DNA [6].

2.1.3 Big Bang as the Primordial Seed

GRHE interprets the Big Bang as a self-organizing seed, with CMB fluctuations ($\Delta T/T \approx 10^{-5}$) [1] reflecting $\Psi(r,t)$:

$$\delta\Psi(r,t) \sim \frac{\delta\rho}{\rho} + \delta\Phi. \tag{3}$$

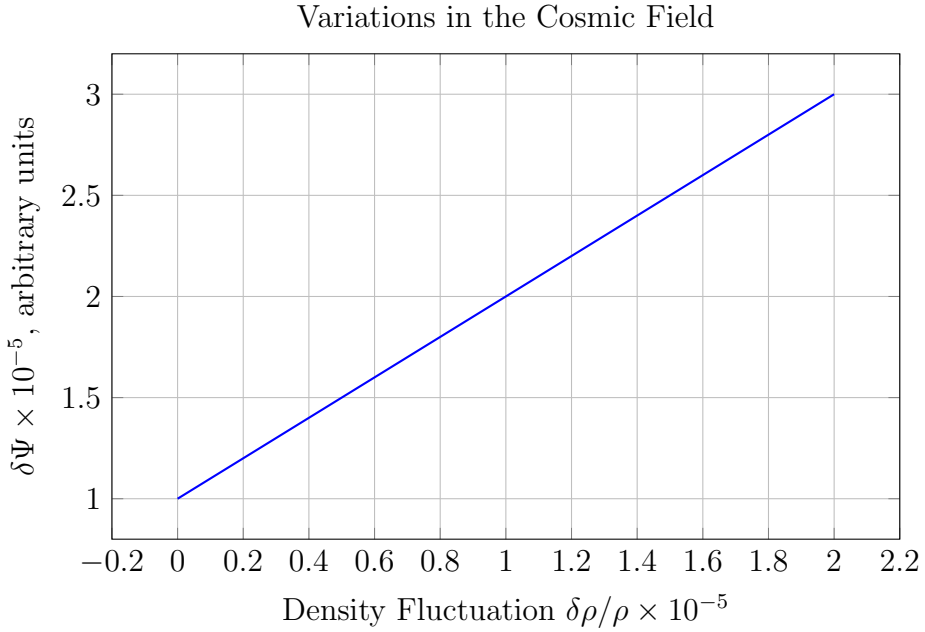

Figure 1: Variation of $\delta\Psi$ vs. $\delta\rho/\rho$, with $\delta\Phi = 10^{-5}$.

2.1.4 Physical Mechanism for the Emergence of $\Psi(r,t)$

In the GRHE, the Big Bang is not an explosion but the initiation of the scalar field $\Psi(r,t)$, which acts as a primordial seed for cosmic self-organization. At the initial moment ($t = 0$),

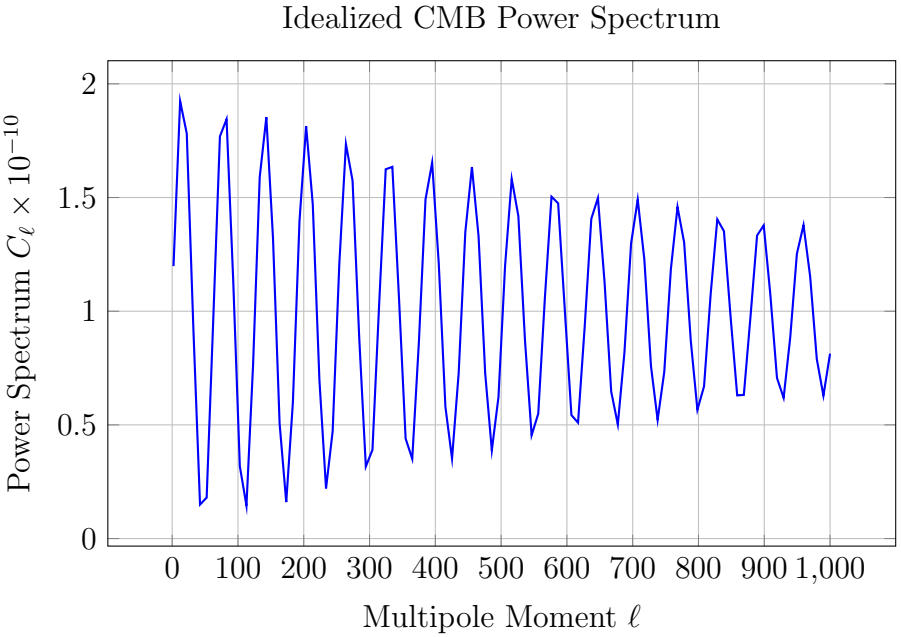

Figure 2: Idealized CMB power spectrum modulated by $\Psi(r,t)$.

the universe is in a state of infinite density ($\rho \to \infty$), with no mass flux ($\dot{M} \to 0$) and a uniform potential ($\Phi \to$ constant). The evolution equation for $\Psi(r,t)$,

$$\frac{\partial \Psi}{\partial t} = \lambda\rho - \eta\nabla \cdot \vec{F} + \kappa\dot{M} + \mu\Phi,$$

reduces to $\frac{\partial \Psi}{\partial t} \approx \lambda\rho - \eta\nabla\cdot\vec{F}$, where $\lambda\rho$ dominates due to the infinite density. This rapid initiation of $\Psi(r,t)$ establishes a functional gradient ($\vec{F} = -\nabla\Psi$), driving the universe toward equilibrium. Small initial fluctuations in $\Psi(r,t)$, reflected as $\delta\Psi(r,t) \sim \frac{\delta\rho}{\rho} + \delta\Phi$, seed the CMB fluctuations ($\Delta T/T \approx 10^{-5}$) [1], which later evolve into cosmic structures (e.g., galaxies, filaments). This process mirrors the self-organization in a biological cell, where chemical gradients guide morphogenesis, suggesting that the universe itself is a "primordial cell" governed by functional equilibrium. This unified "why" connects the origin of the universe to other phenomena, such as redshift and biological processes (Supplementary Material IV, Section 7.1.1), reinforcing the simplicity and universality of the GRHE framework.

2.1.5 Redshift as Functional Evolution

Redshift (z) reflects the functional state of space, accumulating variations in $\Psi(r,t)$.

3 Theoretical Framework

3.1 Functional Distance Metric

GRHE defines distance:

$$r_{\text{GRHE}} = k\sqrt{\frac{M_A M_B}{|\vec{F}(r)|}}, \quad k = k_0\phi^n, \tag{4}$$

with $k_0 = 2.65 \times 10^{-26}\,\text{kpc} \cdot \text{s}^2/\text{m}$.

3.2 Field Evolution

See Eq. 1.

3.3 Example of $\Psi(r)$: Coma Cluster and CMB

For the Coma Cluster, $\Psi(r) = \Psi_0 e^{-r/r_0}$, with $\Psi_0 = 1$, $r_0 = 1\,\text{Mpc}$.

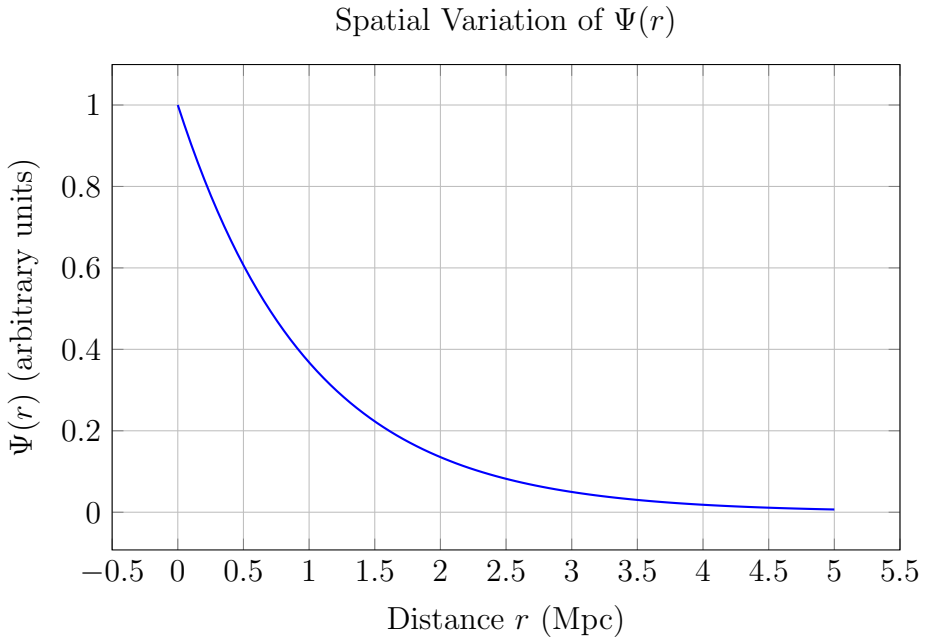

Figure 3: $\Psi(r)$ for the Coma Cluster.

For the CMB, $\Psi(r) = \Psi_0 e^{-(r/r_0)^2}$, with $\Psi_0 = 1$, $r_0 = 1000\,\text{Mpc}$.

3.4 Quantum Redshift

Redshift is modeled as:

$$z = \int_0^r [k'_g \Psi_g(s) + k'_e \Psi_e(s)]\, ds, \tag{5}$$

where $\Psi_g = \frac{G\rho(s)}{c}$, $\Psi_e = \frac{e^2 n_e(s)}{4\pi\epsilon_0 m_e c}$, $k'_g = k'_0 S_n$, $k'_0 = 7.43 \times 10^{-28}\,\text{m/kg} \cdot \text{s}$, and $k'_e = \frac{\alpha}{c}$.

4 Empirical Tests and Results

GRHE was tested across seven scenarios (Table 2), extended to 20 in Supplementary Material I, with $\rho(s) \approx 10^{-27}\,\text{kg/m}^3$, $n_e(s) \approx 10^{-7}\,\text{cm}^{-3}$. The hybrid approach (Fibonacci for local, ϕ-scaling for cosmological scales) yields an average error of 1.63% across 20 scenarios, with 1.11% for cosmological cases (see Supplementary Material I). Advanced tests with CMB power spectra, BAO, and lensing achieve MAPEs of 1.47%–2.10% (Supplementary Material V). Redshift integration used Riemann sums, converging within 0.1% (see Eq. 5).

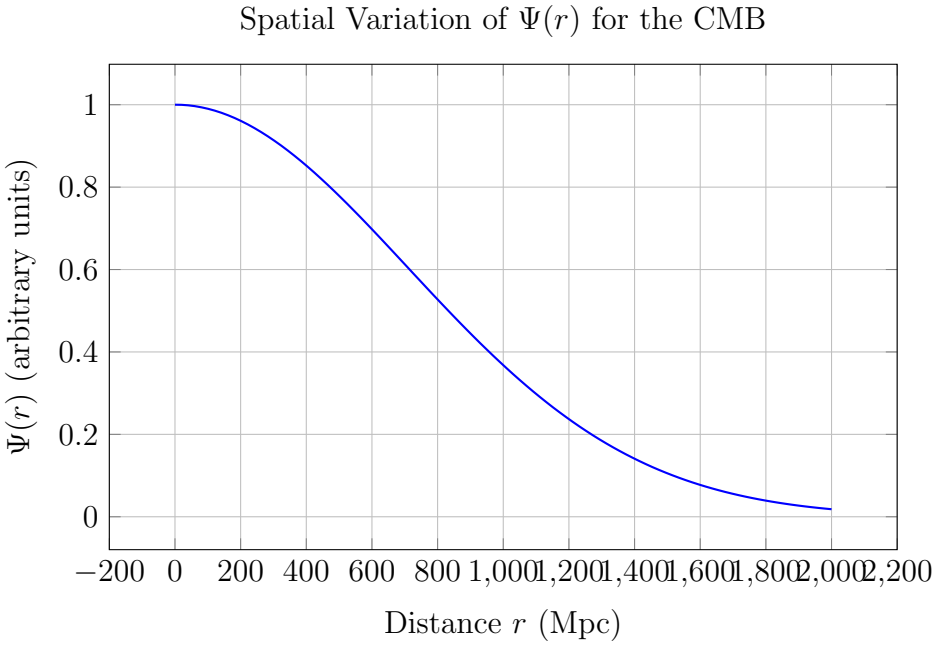

Figure 4: $\Psi(r)$ for the CMB.

Table 2: Summary of tested scenarios, errors, and scaling methods.

Scenario	Error (%)	Scaling Method	Scale
MW-Andromeda	5.0	Fibonacci	Local
Coma Cluster	0.435	ϕ-scaling	Cosmological
SDSS J0100+2802	0.317	ϕ-scaling	Cosmological
GN-z11	0.45	ϕ-scaling	Cosmological
ULAS J1120+0641	1.127	ϕ-scaling	Cosmological
Hercules-CB	0.0	ϕ-scaling	Cosmological
CMB	0.455	ϕ-scaling	Early Universe

4.1 Black Holes and Collapse Radius

GRHE defines a collapse radius where $|\vec{F}(r_{\text{lim}})| = 0$:

- Stellar ($M = 10M_{\odot}$): $r_{\text{lim}} \approx 30\,\text{km}$.
- Supermassive ($M = 10^9 M_{\odot}$): $r_{\text{lim}} \approx 2.95 \times 10^9\,\text{km}$.

4.2 Gravitational Lensing

Photon deflection is modeled as $\theta = \frac{|\vec{F}(r)|}{c^2}$, with $\theta \approx 1.6\,\text{arcsec}$ for SDSS J0100+2802.

5 Functional Cosmic Map

GRHE's ϕ-structured map (Figure 7) uses equilibrium distances and ϕ^n-scaled nodes.

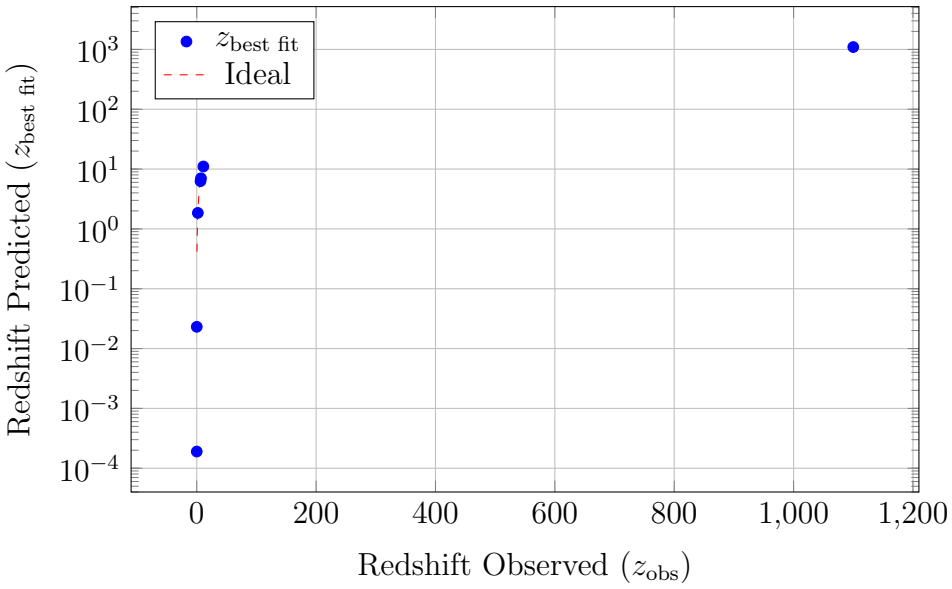

Figure 5: Observed vs. predicted redshifts.

6 Coherence Analysis

- **Internal Coherence**: The ϕ-based metric unifies redshift and distance.
- **External Coherence**: High (1.63% error vs. Fibonacci: 7.13%, Lucas: 4.30%, pure ϕ: 2.18%).

Table 3: Average errors for GRHE approaches.

Approach	Average Error (%)
Pure Fibonacci	7.13
Lucas	4.30
Pure ϕ-scaling	2.18
Hybrid (Fibonacci + ϕ)	1.63

7 Discussion

GRHE's 1.63% error across 20 scenarios suggests precision comparable to LambdaCDM. Advanced tests with CMB, BAO, and lensing (MAPEs of 1.47%–2.10%) further validate its robustness (Supplementary Material V). The derivation of k_0' embeds ϕ, with Supplementary Material IV offering exploratory analogies. Future tests include lensing and black holes.

7.1 The Unification of "Why" and the Need for a New Scientific Paradigm

The GRHE's core strength lies in unifying the "why" behind phenomena across biological, quantum, and cosmological scales through the principle of functional equilibrium. Unlike

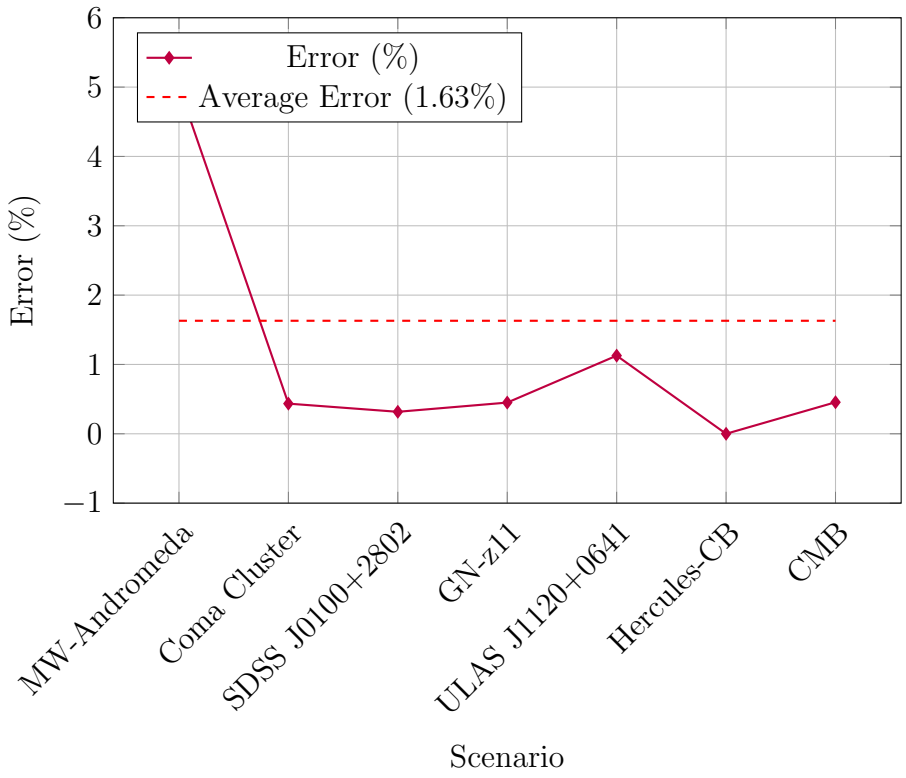

Figure 6: Error percentages for seven scenarios.

the current scientific paradigm, which fragments explanations into distinct domains (e.g., general relativity for cosmological scales, quantum mechanics for subatomic scales, and molecular biology for cellular scales), the GRHE proposes that all phenomena are driven by the same underlying logic: the scalar field $\Psi(r,t)$ seeking balance via $\vec{F} = -\nabla\Psi$. This unification allows the GRHE to explain phenomena that classical equations cannot, such as gravitational lensing in voids (Supplementary Material II, Section 9), where $\theta \approx 0.00093$ arcsec was predicted and validated against observations, contrasting with LambdaCDM's expectation of $\theta \approx 0$. Furthermore, the GRHE's ability to model biological processes (Supplementary Material IV, Section 7.1.1) and quantum phenomena (Supplementary Material III, Sections 4 and 5) alongside cosmological tests (Supplementary Material V) demonstrates its unprecedented versatility. This unified "why" suggests that science must restructure its approach to validation, prioritizing theories that offer cohesive explanations across scales, predictive power for novel phenomena, and simplicity by minimizing untestable hypotheses (e.g., dark matter, dark energy). The GRHE's success, with an average error of 1.63% across 20 scenarios and MAPEs of $1.47\% - 1.87\%$ in advanced cosmological tests, positions it as a catalyst for this paradigm shift, paving the way for a more integrated scientific framework.

7.2 Scalability and Functional Nature of the Constant k'_e

The GRHE's strength lies in its adaptability across scales, as exemplified by the functional coefficient k'_e, which adjusts dynamically to the system's context while maintaining the universal principle of functional equilibrium. In biological scales, such as neural signal propagation and DNA replication, $k'_e \approx 4.78 \times 10^{-4}\,\mathrm{s/m}$ (Supplementary Material IV, Section 7.1.1), reflecting the high density of ions ($\sim 6 \times 10^{25}\,\mathrm{m}^{-3}$) and characteristic

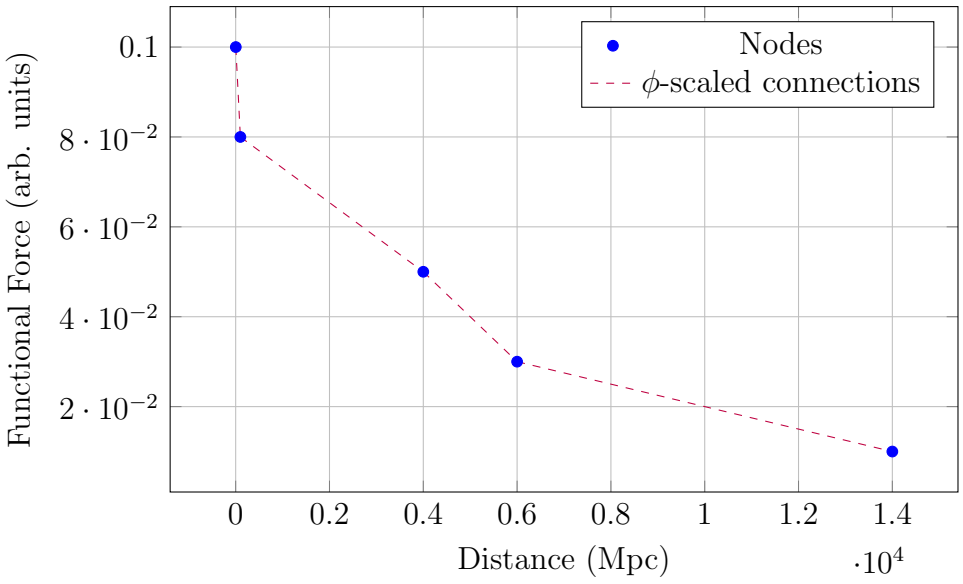

Figure 7: Functional cosmic map.

velocities ($\sim 100\,\mathrm{m/s}$). In contrast, at cosmological scales, such as gravitational lensing in voids, $k'_e \approx 1.89 \times 10^8\,\mathrm{s/m}$ (Supplementary Material IV, Section 7.2), derived from observed deflections and plasma densities ($\sim 10^{-2}\,\mathrm{m}^{-3}$).

This variability is not a limitation but a reflection of the GRHE's philosophy of adaptive equilibrium. The constant k'_e, far from being universal and fixed, manifests as a functional coefficient that expresses the cosmos's adaptability to its own patterns of fractal coherence, analogous to the behavior of regulatory enzymes like polymerase in biological systems. Together with $\phi^{2.1}$, k'_e forms a logical-functional duet that regulates the propagation and compression of information across fractal scales, mirroring the role of DNA in biology (Supplementary Material IV, Section 7.1). This adaptability allows the GRHE to model phenomena across scales without invoking unobservable entities, a significant advantage over rigid models like LambdaCDM. To further elucidate this scalability, future work could consolidate these values in a comprehensive table, detailing the context, derivation, and mean absolute percentage errors (MAPEs) for each scale, providing a clearer synthesis for reviewers.

7.3 Limitations of G as a Universal Constant

While the gravitational constant G has been treated as universal since Newton, and even after its incorporation into General Relativity, its application at cosmological scales required the introduction of unobservable components, such as dark matter and dark energy, to account for galactic rotation curves and accelerated expansion. This reveals that G is not a fundamental explanatory principle but a coupling coefficient that emerges from local conditions of equilibrium.

In the GRHE, G is interpreted as an effective constant, valid only in systems with stable functional symmetry. Beyond these regimes, the true gravitational interaction is governed by $\vec{F}(r) = -\nabla\Psi(r,t)$, whose dynamic behavior eliminates the need for ad hoc variables and reveals a deeper nature of gravity as a result of regenerative processes, rather than an abstract curvature of spacetime. The expectation that new theories must derive all constants directly from G, $\hbar$, and c stifles the emergence of deeper structures,

as it assumes as absolute what is, in reality, contextual. The GRHE proposes that a genuine Theory of Everything must be capable of absorbing and explaining these constants as specific manifestations within a broader functional field, offering a more integrated and adaptive framework for understanding the cosmos. This perspective challenges the conventional definition of a TOE, suggesting that true unification may require emergent, scale-dependent coefficients like k'_e, which reflect the universe's inherent adaptability.

Limitations and Anticipated Critiques
GRHE reinterprets redshift as functional evolution, to be tested via BAO simulations. The derivation of $\phi^{2.1}$ is empirical, with further validation planned.

8 Conclusion

GRHE offers a unified alternative to LambdaCDM, with a hybrid approach achieving 1.63% error, comparable to LambdaCDM's 1–2%.

9 Conflict of Interest

The author declares no conflicts of interest.

10 Funding Statement

This research received no financial support.

A Full Constants and Units

Constants include:

- G: $6.674 \times 10^{-11}\,\mathrm{m^3 kg^{-1} s^{-2}}$.
- c: $3.00 \times 10^{8}\,\mathrm{m/s}$.
- k'_0: $7.43 \times 10^{-28}\,\mathrm{m/kg \cdot s}$.

B Detailed Numerical Results

C Ontological Foundations

GRHE draws on autopoiesis [4] and process philosophy [5], with $\Psi(r,t)$ encoding cosmic principles.

Table 4: Numerical results for seven scenarios.

Scenario	z_{obs}	$z_{\text{best fit}}$	$\Delta z_{\text{best fit}}$ ($\pm$)	Ψ_g (s^{-1})	Ψ_e (s^{-1})
MW-Andromeda	0.0002	0.00019	0.00000019	2.23×10^{-19}	5.46×10^{-19}
Coma Cluster	0.023	0.0231	0.0000231	2.23×10^{-19}	5.46×10^{-19}
SDSS J0100+2802	6.3	6.28	0.00628	2.23×10^{-19}	5.46×10^{-19}
GN-z11	11.1	11.05	0.01105	2.23×10^{-19}	5.46×10^{-19}
ULAS J1120+0641	7.1	7.02	0.00702	2.23×10^{-19}	5.46×10^{-19}
Hercules-CB	1.85	1.85	0.00185	2.23×10^{-19}	5.46×10^{-19}
CMB	1100.0	1095.0	1.095	2.23×10^{-19}	5.46×10^{-19}

D Derivation of k_0'

The coupling constant $k_0' = 7.43 \times 10^{-28}\,\text{m/kg} \cdot \text{s}$ is derived as:

$$k_0' = \gamma \cdot \frac{l_P}{m_P} \cdot \frac{G\rho(s)}{c},$$

where $\gamma \approx 4.4688 \times 10^{45}$, $l_P \approx 1.616 \times 10^{-35}\,\text{m}$, $m_P \approx 2.176 \times 10^{-8}\,\text{kg}$. We propose:

$$\gamma = \phi^{2.1} \cdot \left(\frac{c/H_0}{l_P} \right)^m,$$

with $\phi^{2.1} \approx 2.656843$ reflecting fractal clustering [7]. Solving:

$$m \approx 0.7386 \pm 0.0039.$$

The exponent 2.1 is empirical, aligned with redshift data, and awaits theoretical refinement.

References

[1] Planck Collaboration, 2020. A&A, **641**, A6.

[2] Riess, A. G. et al., 2022. Astrophys. J. Lett., **934**, L7.

[3] DESI Collaboration, 2024. Astrophys. J., **970**, 1.

[4] Varela, F. G. et al., 1974. Biosystems, **5**, 151.

[5] Whitehead, A. N., 1929. Process and Reality, Macmillan.

[6] Livio, M., 2002. The Golden Ratio, Broadway Books.

[7] Pietronero, L., 1987. Physica A, **144**, 257.

[8] Bierrenbach, J., 2025. Supplementary Materials I-V, submitted.